NO: 129 DECEMBER 2006

VERTICAL TRANSFER OF INFRARED RADIATION IN WATER

Eyvind Aas

Abstract

An infrared heating lamp has been used as the driving force in laboratory experiments simulating the thermohaline circulation of the world ocean. The radiative energy from the lamp absorbed at different depths in the laboratory tank, as well as the possible temperature effects, have been calculated. The results demonstrate that in the laboratory more than 50 % of the infrared radiation is absorbed within the upper 0.01 mm, more than 90 % within the upper 0.1 mm, and more than 99 % within the upper 1 mm, and that evidently most of the heat energy in the surface layer is quickly transported away by other physical processes.

ISBN 82-91885-33-8

1. Introduction

Around the beginning of the twentieth century, when the Swedish scientist Johan Wilhelm Sandström was engaged at the University of Kristiania (today the University of Oslo), he carried out a series of laboratory experiments where the most known result probably is the so-called Sandström theorem (Sandström, 1908):

A closed steady circulation can only be maintained in the ocean if the heat source is situated at a lower level than the cold source.

A hundred years later, during the years 2004-2006, two other Swedes, Anna Kristine Wåhlin and Anna Malin Ericsson, ran similar experiments at the same university in order to prove that Sandström was wrong. Some of the results have been published in Ericsson's master thesis at the Göteborg University (M. Ericsson, 2005) and in a paper submitted to the Journal of Fluid Research (Wåhlin et al., 2006). The general idea behind the experiments was to heat the water in a tank from above by means of a lamp, similar to the Sun's heating of the world ocean, and to see if a steady circulation pattern would appear, similar to the thermohaline circulation in the world ocean.

Such a circulation was in fact observed, and the Sandström theorem has therefore been proved wrong. The present paper is a summary of three technical reports written for Wåhlin, quantifying the energy transfer to the different depths of the water in the tank. The purpose of the paper is to create a collected documentation of the calculations and the applied background data.

2. Methods

2.1. Description of the problem

A heating lamp, radiating mainly in the infrared part of the electromagnetic spectrum, has been placed at a short distance above a tank filled with water in the laboratory. The length of the lamp corresponds approximately to the width of the tank, and it is assumed that all the radiation directed directly from the heat element towards the water or reflected from the reflector of the lamp will reach the surface of the water.

The possible thermophysical processes for the transfer of heat to and from an infinitesimal volume of water at a fixed point in the tank are

1: *molecular diffusion of heat*,
2: *heat conduction*,
3: *turbulent diffusion of heat*,
4: *advective transport of heat, due to movements of the water*,
5: *absorbed infrared radiation emitted by the surrounding waters*,
6: *infrared radiation emitted by the water volume due to the temperature of the water,*
7: *absorbed infrared radiation emitted by the lamp.*

At the surface we may also have the process of

8: *heat loss due to evaporation.*

In practical experiments it will not be possible to distinguish between terms 1, 2, 5 and 6 for a water volume away from the surface. The values for molecular diffusion of heat presented in the literature probably contain all four processes.

In this report only the seventh term above will be considered, and it can be useful to calculate what the resulting temperature increase per time unit would be if the other processes could be neglected. The heat equation would then be simplified to

$$\frac{\partial T}{\partial t} c_p \, \rho \, dx \, dy \, dz = -\frac{dE_d}{dz} dx \, dy \, dz \, , \tag{1a}$$

where x and y are the horizontal axes, z is the vertical axis positive downwards, T is the temperature of the infinitesimal volume $dx\,dy\,dz$, t is time, $c_p \approx 4184$ Joule kg^{-1} K^{-1} is the specific heat of water at constant pressure, $\rho \approx 1000$ kg m^{-3} is the density of water, and E_d is the spectrally integrated downward irradiance. Equation (1a) may be written

$$\frac{\partial T}{\partial t} = -\frac{1}{\rho c_p} \frac{dE_d}{dz} \approx \frac{1}{\rho c_p} \frac{|\Delta E_d|}{|\Delta z|} \, . \tag{1b}$$

If we can calculate the vertical attenuation of E_d, we may then obtain the resulting temperature increase by Eq. (1b). However, we cannot calculate the vertical attenuation of E_d directly, but we have to use the spectrally distributed irradiance $E_{d\lambda}(\lambda)$, where λ is the wavelength of the radiation in air.

The problem will be solved step-wise. Firstly we will calculate the spectral irradiance $E_{b\lambda}(\lambda)$ emitted by the heat element of the lamp (Chapter 3.1), secondly the corresponding downward irradiance $E_{d\lambda}(\lambda, 0+)$ incident at the surface of the water (Chapter 3.2), thirdly we will determine the transmitted irradiance $E_{d\lambda}(\lambda, 0-)$ just beneath the surface (Chapter 3.3) before calculating the vertical attenuation coefficient $K_d(\lambda)$ for our downward irradiance (Chapter 3.4). Finally we integrate the spectral distribution $E_{d\lambda}(\lambda,z)$ over all wavelengths in each selected depth to find the corresponding value of $E_d(z)$ and the resulting increase in temperature (Chapter 3.5).

2.2. The blackbody equations

The heat element of the lamp is assumed to radiate like a blackbody. The spectral distribution $E_{b\lambda}(\lambda)$ of the irradiance emitted from an area unit is then described by *Planck's Law*:

$$E_{b\lambda} = \frac{c_1}{\lambda^5} \frac{1}{e^{\frac{c_2}{\lambda T}} - 1} \tag{2}$$

where the two constants are $c_1 = 3.743 \cdot 10^{-16}$ W m^2 = $3.743 \cdot 10^8$ μm^4 W m^{-2} and $c_2 = 1.4388 \cdot 10^4$ μm K. The unit of the temperature T in Eq. (2) is degrees Kelvin. If we use μm as the wavelength unit, the practical unit for the spectral irradiance distribution $E_{b\lambda}$ will be W m^{-2} μm^{-1}.

The wavelength λ_{max}, where the spectral irradiance distribution obtains its maximum, can be found by differentiating Eq. (2). The result becomes a function of the blackbody temperature T, and is known as *Wien's Displacement Law*:

$$\lambda_{\max} T = 2898 \mu m\ K \tag{3}$$

The integral of Eq. (2) over all wavelengths from 0 to ∞ represents the total blackbody irradiance E_b. It is known as the *Stefan-Boltzmann Law*:

$$E_b = \sigma T^4 \tag{4}$$

where σ = 5.6697 10^{-8} W m^{-2} K^{-4}. For two different outputs E_{b1} and E_{b2} from the lamp the ratio between the corresponding temperatures T_1 and T_2 is determined by

$$\frac{T_1}{T_2} = \left(\frac{E_{b1}}{E_{b2}} \right)^{1/4} \tag{5}$$

2.3. Transmittance of $E_{d\lambda}(\lambda)$ at the air-water interface

While *irradiance* represents the component of radiative energy transported in a direction normal to a selected area unit, and where the radiation may come from all possible direction within a hemisphere, the *radiance* describes the radiation in a certain direction. Radiance is defined as the flux of radiative energy per unit of solid angle and per area unit normal to the ray's direction. Emitted spectral radiance $L_{b\lambda}$ from an area unit in a blackbody is characterized by remaining constant in all possible directions, and it is therefore related to the irradiance $E_{b\lambda}$ by

$$L_{b\lambda} = \frac{E_{b\lambda}}{\pi} \tag{6}$$

Similarly the total spectrally integrated radiance L_b is related to E_b by

$$L_b = \frac{E_b}{\pi} \tag{7}$$

The isotropic properties of the blackbody radiance imply that the direct radiance from the heat element incident at the surface of the water will be constant for all possible directions. The radiance hitting the reflector of the lamp before it is redirected towards the water may be somewhat less isotropic, but for the sake of simplicity we have still assumed that all radiance from the lamp incident at the water is isotropic.

The radiance reflectance is described by the *Fresnel Equations.* For polarized radiance where the electric vector is parallel to the plane of incidence, the reflectance will be

$$\rho_p = \frac{tg^2(i-j)}{tg^2(i+j)} \tag{8}$$

Here i is the angle of incidence of the radiance in air, relative to the zenith, and j is the resulting angle of refraction in water, relative to the nadir. The two angles are related to each other by *Snell's Law*

$$\sin i = n \sin j \tag{9}$$

where n is the refractive index of water relative to air.

For polarized radiance where the electric vector is normal to the plane of incidence, the reflectance will be

$$\rho_n = \frac{\sin^2(i-j)}{\sin^2(i+j)}, \tag{10}$$

while the reflectance of unpolarized radiance is the mean value of the polarized radiances

$$\rho = \frac{1}{2}\left(\rho_p + \rho_n\right) \quad . \tag{11}$$

For radiance of normal incidence ($i = j = 0$) the reflectance becomes, regardless of polarization,

$$\rho_o = \frac{(n-1)^2}{(n+1)^2} \, . \tag{12}$$

Due to the laws of conservation of energy the part of the radiative energy that is not reflected at an interface must be transmitted, and consequently the radiance transmittance τ will be

$$\tau = 1 - \rho \, . \tag{13}$$

In the special case when the radiance in the downward irradiance is isotropic, the irradiance reflectance becomes

$$\rho_{iso} = \frac{\int_0^{\pi/2} \rho(i) \sin i \cos i \, di}{\int_0^{\pi/2} \sin i \cos i \, di} = \int_0^{\pi/2} \rho(i) \sin 2i \, di \tag{14}$$

The corresponding transmittance τ_{iso} for irradiance resulting from an isotropic radiance distribution becomes

$$\tau_{iso} = 1 - \rho_{iso}, \tag{15}$$

and it can be demonstrated analytically that the irradiance $E_{d\lambda}(\lambda, 0-)$ just beneath the surface is related to the irradiance transmittance τ_{iso} and the irradiance $E_{d\lambda}(\lambda, 0+)$ just above the surface by

$$E_{d\lambda}(\lambda, 0-) = \tau_{iso} \, E_{d\lambda}(\lambda, 0+) \tag{16}$$

If the irradiance consists only of radiance of normal incidence, then according to Eq. (12) the corresponding transmittance becomes

$$\tau_o = 1 - \rho_o = \frac{4n}{(n+1)^2}. \tag{17}$$

2.4. Vertical attenuation of $E_{d\lambda}(\lambda, z)$

The vertical attenuation of the downward irradiance $E_{d\lambda}(\lambda, z)$ at the different wavelengths can be approximated as a function of the vertical coordinate z ($z = 0$ at the surface, positive downwards) by

$$E_{d\lambda}(\lambda, z) = E_{d\lambda}(\lambda, 0-) \, e^{-K_d(\lambda) \, z} \tag{18}$$

where $K_d(\lambda)$ is the vertical attenuation coefficient of downward irradiance at the wavelength λ. $K_d(\lambda)$ has been thoroughly investigated in the visible part of the spectrum (*e.g.* Jerlov, 1976), where K_d is determined mainly by organic and inorganic particles and dissolved substances in addition to the pure water. In the visible part the established expression

$$K_d(\lambda) \approx (a + b_b) / \mu_d, \tag{19}$$

where a is the absorption coefficient, b_b the backscattering coefficient and μ_d the average cosine of the downward radiance, offers a good approximation of the vertical attenuation coefficient. The average cosine μ_d is defined as

$$\mu_d = \frac{\int_0^{\pi/2} \overline{L}(j) \sin j \cos j \, dj}{\int_0^{\pi/2} \overline{L}(j) \sin j \, dj}, \tag{20}$$

where $\overline{L}(j)$ is the azimuthal mean value of the radiance in water in the direction of the nadir angle j. When we consider only the incident infrared radiance, which is isotropic and transmitted through the surface by the transmittance τ, the expression for the average cosine μ_d can be written

$$\mu_d = \frac{\int_0^{j_{cr}} \tau(j) \sin j \cos j \, dj}{\int_0^{j_{cr}} \tau(j) \sin j \, dj}. \tag{21}$$

Here the critical angle j_{cr} is defined by $i_{cr} = \pi/2$, so that

$$\sin j_{cr} = \frac{1}{n}. \tag{22}$$

In our case practically all energy lies within the infrared part of the spectrum, where the absorption of pure water will dominate all other contributions to the attenuation. In Eq. (19) we can therefore omit b_b when compared to a without any consequences for our calculated values of the spectrally integrated $E_d(z)$, and we will apply the expression

$$K_d(\lambda) \approx a / \mu_d \tag{23}$$

for the entire spectral range 0.4-100 μm. In some references the absorption index κ is used rather than the absorption coefficient a. The two quantities are related by

$$a = \frac{4\pi\kappa}{\lambda} \tag{24}$$

3. Results

3.1. Irradiance emitted by the lamp

100W
The lamp was a GLAMOX infrared heater type GVR 505G, with the following possible effects: 100-200-300-500 W. While the lamp switch was in the 100 W position the temperature of the heating element was measured by an infrared camera as 320 degrees, or 593 Kelvin. The corresponding spectral irradiance distribution $E_{b\lambda}(\lambda)$ according to Eq. (2) is shown in Fig. 1.

The peak wavelength λ_{max}, determined from Eq. (3), becomes 4.89 µm, and the spectrally integrated irradiance emitted from the surface of the heating element will be $E_b \approx 7010$ W m^{-2} based on Eq. (4). When the emitted irradiance from the heating element is multiplied by its area, the result should become 100 W. The heating element is shaped like a bent tube, with an estimated length of 34 cm and a circumference of 4.1 cm, resulting in a surface area of 0.0139 ± 0.0004 m^2 and a radiated effect of 97.4 ± 2.8 W. The deviation from the nominal 100 W corresponds to the uncertainty of the estimated area.

It is noteworthy that when we numerically integrate the spectral curve described by Eq. (2), the result shows that in this case more than 99 % of the radiative energy is found between 2 and 40 µm.

200 - 300 W
When the lamp's ouput is doubled from 100 to 200 W, the ratio between the corresponding Kelvin temperatures should be 1 : $2^{1/4}$ = 1 : 1.19, according to Eq. (5). The temperature at 200 W has then been estimated to be 593 K x 1.19 = 705 K. Similarly the temperature at 300 W has been estimated as 593 K x $3^{1/4}$ = 780 K. The spectral distributions of the irradiance from the heating element are shown in Fig. 1. When the output is 300 W, more than 98% of the radiative energy is emitted within the wavelength interval 2-40 µm.

3.2. Irradiance incident at the surface of the water

100 W
Not all of the 100 W will be directed towards the surface of the water. The lamp will necessarily absorb some of the heat it produces and will suffer heat loss from its side-walls.

A bimetal thermocouple was soldered to the back of the lamp, and its temperature was read off for the different nominal lamp effects. The position of the lamp was found to have a significant influence on the temperature of the side-walls. If the heating element was pointing upwards, the temperatures would be 60-80 degrees lower than when the element was pointing in its normal downward direction. In the latter position the temperature would be around 358 Kelvin for an 100 W effect. By using Eq. (4) and multiplying it by the area of the side-walls, 0.0612 m^2 excluding the area of the reflector, the heat loss was estimated to be 29.7 W. Thus 70.3 W is assumed to reach the surface of the water in the tank when the nominal effect is 100 W. The area of the water irradiated by the lamp has been estimated to be 0.040 m^2 (width across tank 0.40 m and length along tank 0.1 m), and the irradiance then becomes 70.3 W / 0.040 m^2 = 1760 W m^{-2}. The spectral distribution $E_{d\lambda}(\lambda, 0+)$ of this irradiance is presented in Fig. 2.

200 - 300 W

The temperatures at the back of the lamp were around 375 and 391 K for 200 and 300 W, respectively, and the corresponding heat losses have been estimated at 41.6 and 53.7 W. The corresponding infrared irradiances incident at the surface of the water become 3960 and 6160 W m^{-2}, respectively. Their spectral distributions are presented in Fig. 2.

3.3. Irradiance just beneath the surface

Our basic assumption for the incident infrared radiance from the lamp is that it is isotropic. The reflectance ρ_{iso} (Eq. 14) of the corresponding irradiance at the air-water interface is presented as a function of the refractive index of water, n, in Fig. 3. An accurate relationship, valid for n in the interval 1.1-2, is

$$\rho_{iso} \approx -0.0305n^2 + 0.2432n - 0.2043 \tag{25}$$

The refractive index n as a function of wavelength is shown in Fig. 4 and Table 1. The data for the wavelength interval 0.4-1.25 μm are taken from Lauscher (1955), and for the interval 1.25-100 μm from Zoloratev & Demin (1977). The total range of n in the spectral domain 0.4-100 μm is 1.116-1.985, but in the smaller domain 2-40 μm, which contains more than 98 % of the energy, the variation is 1.116-1.550.

The resulting values for τ_{iso} (Eq. 15) vary between 0.90 and 0.97 in the spectral range 2-40 μm (Fig. 5, Table 1). This implies that if we had chosen a constant value for τ_{iso} equal to 0.935, the average deviation within this spectral range would be less than 4 %. The transmittances of the spectrally integrated irradiances vary even less and become 0.939, 0.938 and 0.937 for 100, 200 and 300 W, respectively.

For a radiance of normal incidence against the surface of the water rather than the assumed isotropic distribution, the irradiance transmittance τ_o (Eq. 17) would obtain values from 0.953 to 0.998 for the spectral domain 2-40 μm (Table 1). This result indicates that the directions of the incident infrared radiance have no crucial influence on the magnitude of the transmitted irradiance. The spectral distribution of the transmitted irradiance is shown in Fig. 6.

3.4. The vertical attenuation coefficient of downward irradiance

The vertical attenuation coefficient $K_d(\lambda)$ for downward irradiance was calculated by means of Eq.(23). We have applied values of a for pure water, even if the water in the tank is not particularly clean. This can be justified because the contribution from pure water to the absorption coefficient dominates all the other contributions in the infrared part of the spectrum. The values for a come from Pope & Fry (1997) for the wavelength interval 0.4-0.72 μm, from Curcio & Petty (1951) for the range 0.72-2.5 μm, and from Zoloratev & Demin (1978) for 2.5-100 μm. The applied values of a are shown in Fig. 7 and Table 1.

The average cosine μ_d of the transmitted infrared radiance was calculated by Eq. (21), and the result is presented as a function of n in Fig. 8. The function can be approximated by the polynomial

$$\mu_d = -0.5987n^4 + 4.1282n^3 - 10.744n^2 + 12.636n - 4.7927 \qquad (26)$$

The spectral variation of μ_d is displayed by Fig. 9 and Table 1. The range of μ_d is 0.73-0.94 with a mean value of 0.84 for the spectral domain 0.4-100 μm. For the domain 2-40 μm the range becomes 0.73-0.89 with the mean value 0.82.

The vertical attenuation coefficient $K_d(\lambda)$ can now be calculated by Eq. (23). Fig. 10 and Table 1 demonstrate that $K_d(\lambda)$ varies by more than 8 decades through the spectrum. The minimum occurs close to the violet wavelength 0.4 μm with a $K_d(\lambda)$ of 0.008 m^{-1}. The maximum is found in the infrared around 3 μm with a $K_d(\lambda)$ of $1.5 \cdot 10^6$ m^{-1}.

3.5. Integrated irradiance E_d at different depths and the corresponding increase in temperature

At the depth z = 1 μm the spectral downward irradiance at the wavelength 3 μm has been reduced to 22 % of its value just beneath the surface. Although this is the wavelength of the maximum vertical attenuation, the example shows that the infrared radiation will be absorbed within a very thin upper layer. Consequently it will be difficult to present the vertical attenuation of the spectral irradiance in a readable graphic manner. It is more instructive to calculate $E_{d\lambda}(\lambda)$ for the different wavelengths at the different depths, integrate the spectral distribution, and then present the obtained values of $E_d(z)$, as shown by Fig. 11 and Table 2. The corresponding temperature increase may then be calculated for the different layers by Eq. (1b). The integrations were performed with $\Delta\lambda$ = 0.05 μm in the wavelength interval 0.4-7.0 μm, $\Delta\lambda$ = 0.1 μm in the interval 7.0-13 μm, $\Delta\lambda$ = 0.2 μm in the interval 13-15 μm, $\Delta\lambda$ = 0.5 μm in the interval 15-20 μm, and $\Delta\lambda$ = 1 μm in the interval 20-100 μm. The results are presented in Table 3.

Table 2 shows that 57-66 % of the radiative energy will be absorbed in the layer 0-0.01 mm, 93-97 % in the layer 0-0.1 mm, and 99.3-99.9 % in the layer 0-1 mm, when the nominal lamp effectslie in the range from 100 to 300 W. According to Table 3 the average value of $\partial T/\partial t$ will be 23-71 degrees per second within the upper 0.01 mm, depending on the lamp output, meaning that the water should start boiling within 4 seconds if there were no heat transports away from this layer. If we look at the average temperature increase within the upper 0-0.1 mm, the numbers become 3.8-12.8 degrees per second, and the average values within the upper 1 mm are 0.4-1.4 degrees per second. Since neither boiling nor the estimated increases in temperature are observed, it follows that the terms that were omitted in Eq. (1b) have a significant influence on the heat budget. The details of the laboratory experiments have been discussed by Ericsson (2004) and Wåhlin et al. (2006).

3.6. Scaling ratio between the oceanic conditions and the experiment

Fig. 11 shows that 1 % of the irradiance just beneath the surface remains at the depths 0.2, 0.4 and 0.7 mm for the lamp's output at 100, 200 and 300 W, respectively, implying that 99 % has been absorbed between the surface and the mentioned depths. In the tropical regions the ocean waters are very clear, and based on the optical properties of Jerlov's oceanic water types *I-III*, the 1 % depth may be found between 25 and 90 m (e.g. Jerlov, 1976). Similar numbers for a 50 % level can be found for the laboratory set-up and the world ocean. The results are presented in Table 4. The vertical extensions of the currents forming the thermohaline circulation are also shown in the table.

The ratios between the vertical scales of the currents in the world ocean and the tank experiment lie in the range 10^4-10^5, while the ratio for the scales of the penetration depths are seen to be slightly greater, up to a factor of 10. This is a very satisfactory and fortuitous result, considering that the temperatures of the lamp's heating element and the resulting spectral distributions were not known before these experiments started.

Acknowledgement

Our thanks are due to Knut Jørgen Måløy and Torfinn Lindem, both at the Department of Physics, for supplying the infrared camera and the thermocouple.

References

Curcio, J. A., & Petty, C. C., 1951. The near infrared absorption spectrum of liquid water. *J. Opt. Soc. Am.*, **41**: 302-304.

Ericsson, M., 2005. The upper ocean circulation - A laboratory experiment. Thesis, Earth Sciences Centre, Göteborg University, Sweden.

Jerlov, N. G., 1976. *Marine optics*. Elsevier, Amsterdam. 231 pp.

Lauscher, F., 1955. Sonnen- und Himmelsstrahlung im Meer und in Gewässern. In: *Handbuch der Geophysik*. Springer, Berlin-Heidelberg-Wien, **8**: 723-768.

Pope, R. M., & Fry, E. S., 1997. Absorption spectrum (380-700 nm) of pure water. II. Integrating cavity measurements. *Appl. Opt.*, **36**: 8710-8723.

Sandström, J. W., 1908. Dynamische Versuche mit Meerwasser. *Annalen der Hydrographie und Maritimen Meteorologie*, Vol 36, pp. 6-23.

Wåhlin, A. K., Ericsson, A. M., Aas, E., Broström, G., Weber, J. E., and Grue, J., 2006. Horizontal convection in water heated by infrared radiation and cooled by evaporation. Part I. Experimental results and scaling analysis. Submitted to JFM.

Zoloratev, V. M., & Demin, A. V., 1977. Optical constants of water over a broad range of wavelengths, 0.1 Å - 1 m. *Opt. Spectrosc.*, **43**: 157-161(U.S. version).

Table 1. Spectral values of applied optical quantities

λ [μm]	n	τ_{iso}	τ_o	a [m-1]	μ_d	K_d [m^{-1}]
0.4	1.3433	0.9326	0.9785	0.00663	0.8432	0.007863
0.45	1.3390	0.9333	0.9790	0.00922	0.8418	0.01095
0.5	1.3360	0.9338	0.9793	0.0204	0.8409	0.02426
0.55	1.3345	0.9341	0.9795	0.0565	0.8404	0.06723
0.6	1.3325	0.9344	0.9797	0.2224	0.8398	0.2648
0.65	1.3310	0.9346	0.9798	0.34	0.8393	0.4051
0.7	1.3300	0.9348	0.9799	0.624	0.8390	0.7438
0.75	1.3295	0.9349	0.9800	2.5	0.8388	2.98
0.8	1.3280	0.9351	0.9801	2	0.8383	2.386
0.85	1.3275	0.9352	0.9802	4.2	0.8381	5.011
0.9	1.3260	0.9354	0.9804	7	0.8377	8.357
0.95	1.3255	0.9355	0.9804	45	0.8375	53.73
1	1.3247	0.9357	0.9805	37	0.8372	44.19
1.05	1.3240	0.9358	0.9806	13	0.8370	15.53
1.1	1.3230	0.9359	0.9807	20	0.8367	23.9
1.15	1.3220	0.9361	0.9808	80	0.8363	95.66
1.2	1.3215	0.9362	0.9808	105	0.8362	125.6
1.25	1.3210	0.9363	0.9809	90	0.8360	107.7
1.3	1.3225	0.9360	0.9807	105	0.8365	125.5
1.35	1.3220	0.9361	0.9808	250	0.8363	298.9
1.4	1.3210	0.9363	0.9809	1230	0.8360	1471
1.45	1.3200	0.9364	0.9810	2600	0.8357	3111
1.5	1.3190	0.9366	0.9811	1874	0.8353	2243
1.55	1.3180	0.9367	0.9812	990	0.8350	1186
1.6	1.3160	0.9371	0.9814	650	0.8343	779.1
1.65	1.3140	0.9374	0.9816	500	0.8336	599.8
1.7	1.3125	0.9376	0.9817	520	0.8331	624.2
1.75	1.3110	0.9379	0.9819	650	0.8326	780.7
1.8	1.3090	0.9382	0.9821	800	0.8319	961.7
1.85	1.3070	0.9385	0.9823	900	0.8312	1083
1.9	1.3055	0.9388	0.9824	8000	0.8306	9631
1.95	1.3055	0.9388	0.9824	11400	0.8306	13720
2	1.3020	0.9394	0.9828	6700	0.8294	8078
2.05	1.3000	0.9397	0.9830	4200	0.8286	5068
2.1	1.2900	0.9413	0.9840	2600	0.8249	3152
2.15	1.2800	0.9430	0.9849	1920	0.8211	2338
2.2	1.2770	0.9435	0.9852	1600	0.8199	1952
2.25	1.2700	0.9446	0.9859	1730	0.8171	2117
2.3	1.2650	0.9455	0.9863	2200	0.8150	2699
2.35	1.2600	0.9463	0.9868	3160	0.8129	3887
2.4	1.2570	0.9468	0.9870	4330	0.8116	5335
2.45	1.2600	0.9463	0.9868	6000	0.8129	7381
2.5	1.2620	0.9460	0.9866	8550	0.8137	10510

Table 1 (cont.)

λ [μm]	n	τ_{iso}	τ_o	a [m-1]	μ_d	K_d [m^{-1}]
2.55	1.2500	0.9480	0.9877	15300	0.8085	18920
2.6	1.2300	0.9513	0.9894	24000	0.7993	30030
2.65	1.2140	0.9540	0.9907	33668	0.7914	42540
2.7	1.1670	0.9620	0.9941	83776	0.7650	109500
2.75	1.1340	0.9677	0.9961	237619	0.7434	319600
2.8	1.1165	0.9708	0.9970	581018	0.7308	795000
2.85	1.1590	0.9634	0.9946	934603	0.7600	1230000
2.9	1.2260	0.9520	0.9897	1204548	0.7974	1511000
2.95	1.3125	0.9376	0.9817	1267308	0.8331	1521000
3	1.3870	0.9257	0.9737	1177133	0.8556	1376000
3.05	1.4370	0.9178	0.9678	1021790	0.8675	1178000
3.1	1.4685	0.9129	0.9640	867599	0.8741	992600
3.15	1.4840	0.9106	0.9620	598557	0.8771	682400
3.2	1.4820	0.9109	0.9623	416261	0.8767	474800
3.25	1.4670	0.9132	0.9642	301593	0.8738	345200
3.3	1.4470	0.9163	0.9666	203758	0.8697	234300
3.35	1.4330	0.9184	0.9683	148454	0.8666	171300
3.4	1.4180	0.9208	0.9701	103488	0.8632	119900
3.45	1.4080	0.9223	0.9713	65564	0.8608	76160
3.5	1.3990	0.9238	0.9723	46675	0.8586	54360
3.55	1.3910	0.9250	0.9733	24071	0.8566	28100
3.6	1.3860	0.9258	0.9738	17310	0.8553	20240
3.65	1.3800	0.9268	0.9745	15180	0.8537	17780
3.7	1.3745	0.9276	0.9751	13252	0.8522	15550
3.75	1.3700	0.9284	0.9756	11704	0.8510	13750
3.8	1.3670	0.9288	0.9760	10942	0.8501	12870
3.85	1.3620	0.9296	0.9765	10445	0.8487	12310
3.9	1.3570	0.9304	0.9771	11570	0.8473	13660
3.95	1.3530	0.9311	0.9775	12900	0.8461	15250
4	1.3490	0.9317	0.9779	13817	0.8449	16350
4.05	1.3450	0.9324	0.9784	15372	0.8437	18220
4.1	1.3420	0.9329	0.9787	17164	0.8428	20370
4.15	1.3400	0.9332	0.9789	18250	0.8421	21670
4.2	1.3390	0.9333	0.9790	19882	0.8418	23620
4.25	1.3380	0.9335	0.9791	21880	0.8415	26000
4.3	1.3360	0.9338	0.9793	24490	0.8409	29120
4.35	1.3350	0.9340	0.9794	26272	0.8406	31260
4.4	1.3340	0.9341	0.9795	28060	0.8402	33400
4.45	1.3320	0.9345	0.9797	32400	0.8396	38590
4.5	1.3315	0.9346	0.9798	34746	0.8394	41390
4.55	1.3310	0.9346	0.9798	37090	0.8393	44190
4.6	1.3310	0.9346	0.9798	39686	0.8393	47290
4.65	1.3310	0.9346	0.9798	40990	0.8393	48840
4.7	1.3310	0.9346	0.9798	41411	0.8393	49340
4.75	1.3310	0.9346	0.9798	40979	0.8393	48830
4.8	1.3310	0.9346	0.9798	40055	0.8393	47730
4.85	1.3305	0.9347	0.9799	37980	0.8391	45260
4.9	1.3300	0.9348	0.9799	35904	0.8390	42800
4.95	1.3295	0.9349	0.9800	33660	0.8388	40130

Table 1 (cont.)

λ [µm]	n	τ_{iso}	τ_o	a [m-1]	μ_d	K_d [m^{-1}]
5	1.3290	0.9350	0.9800	31416	0.8386	37460
5.05	1.3280	0.9351	0.9801	28767	0.8383	34320
5.1	1.3270	0.9353	0.9803	26118	0.8380	31170
5.15	1.3240	0.9358	0.9806	24750	0.8370	29570
5.2	1.3220	0.9361	0.9808	23390	0.8363	27970
5.25	1.3190	0.9366	0.9811	23220	0.8353	27800
5.3	1.3155	0.9372	0.9814	23000	0.8341	27570
5.35	1.3110	0.9379	0.9819	23000	0.8326	27630
5.4	1.3070	0.9385	0.9823	24000	0.8312	28880
5.45	1.3040	0.9390	0.9826	25000	0.8301	30120
5.5	1.3020	0.9394	0.9828	26500	0.8294	31950
5.55	1.2990	0.9398	0.9831	28500	0.8283	34410
5.6	1.2900	0.9413	0.9840	32000	0.8249	38790
5.65	1.2820	0.9426	0.9847	37800	0.8219	45990
5.7	1.2750	0.9438	0.9854	45000	0.8191	54940
5.75	1.2650	0.9455	0.9863	54636	0.8150	67040
5.8	1.2530	0.9475	0.9874	71000	0.8098	87670
5.85	1.2450	0.9488	0.9881	102175	0.8063	126700
5.9	1.2410	0.9495	0.9884	138000	0.8045	171500
5.95	1.2480	0.9483	0.9878	179097	0.8076	221800
6	1.2680	0.9450	0.9860	212202	0.8162	260000
6.05	1.2910	0.9412	0.9839	238191	0.8253	288600
6.1	1.3180	0.9367	0.9812	263688	0.8350	315800
6.15	1.3437	0.9326	0.9785	216453	0.8433	256700
6.2	1.3544	0.9309	0.9773	173991	0.8465	205500
6.25	1.3550	0.9308	0.9773	134712	0.8467	159100
6.3	1.3481	0.9319	0.9780	117518	0.8446	139100
6.35	1.3420	0.9329	0.9787	103240	0.8428	122500
6.4	1.3370	0.9337	0.9792	93337	0.8412	111000
6.45	1.3340	0.9341	0.9795	78595	0.8402	93540
6.5	1.3310	0.9346	0.9798	65521	0.8393	78070
6.55	1.3280	0.9351	0.9801	63960	0.8383	76300
6.6	1.3250	0.9356	0.9805	62625	0.8373	74790
6.65	1.3240	0.9358	0.9806	61629	0.8370	73630
6.7	1.3220	0.9361	0.9808	60900	0.8363	72820
6.75	1.3205	0.9363	0.9809	60500	0.8358	72380
6.8	1.3185	0.9367	0.9811	60100	0.8351	71960
6.85	1.3170	0.9369	0.9813	59621	0.8346	71430
6.9	1.3160	0.9371	0.9814	59000	0.8343	70720
6.95	1.3140	0.9374	0.9816	58250	0.8336	69880
7	1.3130	0.9376	0.9817	57550	0.8333	69070
7.1	1.3105	0.9380	0.9819	56700	0.8324	68120
7.2	1.3080	0.9384	0.9822	56100	0.8315	67470
7.3	1.3060	0.9387	0.9824	55500	0.8308	66800
7.4	1.3035	0.9391	0.9826	54850	0.8299	66090
7.5	1.3015	0.9394	0.9828	54400	0.8292	65610
7.6	1.2990	0.9398	0.9831	54100	0.8283	65320
7.7	1.2970	0.9402	0.9833	53900	0.8275	65130
7.8	1.2940	0.9407	0.9836	53800	0.8264	65100
7.9	1.2915	0.9411	0.9838	53800	0.8255	65170

Table 1 (cont.)

λ [μm]	n	τ_{iso}	τ_o	a [m-1]	μ_d	K_d [m^{-1}]
8	1.2880	0.9417	0.9842	53900	0.8242	65400
8.1	1.2850	0.9422	0.9844	54100	0.8230	65730
8.2	1.2820	0.9426	0.9847	54250	0.8219	66010
8.3	1.2805	0.9429	0.9849	54250	0.8213	66060
8.4	1.2795	0.9431	0.9850	54250	0.8209	66090
8.5	1.2770	0.9435	0.9852	54350	0.8199	66290
8.6	1.2720	0.9443	0.9857	54650	0.8179	66820
8.7	1.2660	0.9453	0.9862	54900	0.8154	67330
8.8	1.2605	0.9462	0.9867	55300	0.8131	68010
8.9	1.2565	0.9469	0.9871	55900	0.8114	68900
9	1.2525	0.9475	0.9874	56000	0.8096	69170
9.1	1.2485	0.9482	0.9878	56000	0.8079	69320
9.2	1.2450	0.9488	0.9881	56800	0.8063	70450
9.3	1.2400	0.9496	0.9885	57500	0.8040	71520
9.4	1.2345	0.9506	0.9890	58000	0.8014	72370
9.5	1.2300	0.9513	0.9894	58750	0.7993	73500
9.6	1.2250	0.9521	0.9898	59500	0.7969	74670
9.7	1.2220	0.9527	0.9900	60500	0.7954	76060
9.8	1.2180	0.9533	0.9903	62191	0.7934	78390
9.9	1.2120	0.9543	0.9908	65700	0.7903	83130
10	1.2060	0.9554	0.9913	70372	0.7872	89390
10.1	1.2000	0.9564	0.9917	76300	0.7840	97320
10.2	1.1950	0.9572	0.9921	82544	0.7813	105700
10.3	1.1910	0.9579	0.9924	87000	0.7791	111700
10.4	1.1870	0.9586	0.9927	91500	0.7768	117800
10.5	1.1810	0.9596	0.9931	99000	0.7734	128000
10.6	1.1740	0.9608	0.9936	107881	0.7692	140200
10.7	1.1700	0.9615	0.9939	112500	0.7668	146700
10.8	1.1670	0.9620	0.9941	116400	0.7650	152200
10.9	1.1630	0.9627	0.9943	121052	0.7625	158800
11	1.1675	0.9619	0.9940	129000	0.7653	168600
11.1	1.1520	0.9646	0.9950	136985	0.7555	181300
11.2	1.1480	0.9653	0.9953	142500	0.7529	189300
11.3	1.1450	0.9658	0.9954	148000	0.7509	197100
11.4	1.1410	0.9665	0.9957	154324	0.7482	206300
11.5	1.1350	0.9676	0.9960	165000	0.7441	221700
11.6	1.1300	0.9684	0.9963	176579	0.7406	238400
11.7	1.1265	0.9690	0.9965	185000	0.7381	250600
11.8	1.1230	0.9697	0.9966	193000	0.7356	262400
11.9	1.1200	0.9702	0.9968	201696	0.7334	275000
12	1.1180	0.9705	0.9969	212000	0.7319	289700
12.1	1.1170	0.9707	0.9969	223000	0.7312	305000
12.2	1.1160	0.9709	0.9970	233817	0.7304	320100
12.3	1.1170	0.9707	0.9969	245000	0.7312	335100
12.4	1.1180	0.9705	0.9969	256000	0.7319	349800
12.5	1.1200	0.9702	0.9968	266407	0.7334	363300
12.6	1.1230	0.9697	0.9966	277500	0.7356	377300
12.7	1.1270	0.9690	0.9964	288000	0.7385	390000
12.8	1.1310	0.9683	0.9962	297470	0.7413	401300
12.9	1.1350	0.9676	0.9960	305000	0.7441	409900

Table 1 (cont.)

λ [µm]	n	τ_{iso}	τ_o	a [m-1]	μ_d	K_d [m^{-1}]
13	1.1385	0.9670	0.9958	310000	0.7465	415300
13.2	1.1480	0.9653	0.9953	322727	0.7529	428700
13.4	1.1640	0.9625	0.9943	340000	0.7631	445500
13.6	1.1800	0.9598	0.9932	352000	0.7728	455500
13.8	1.1950	0.9572	0.9921	358000	0.7813	458200
14	1.2100	0.9547	0.9910	364000	0.7893	461200
14.2	1.2250	0.9521	0.9898	369000	0.7969	463100
14.4	1.2400	0.9496	0.9885	372500	0.8040	463300
14.6	1.2590	0.9465	0.9869	373500	0.8124	459700
14.8	1.2750	0.9438	0.9854	373500	0.8191	456000
15	1.2880	0.9417	0.9842	371000	0.8242	450100
15.5	1.3200	0.9364	0.9810	369000	0.8357	441600
16	1.3550	0.9308	0.9773	364000	0.8467	429900
16.5	1.3825	0.9264	0.9742	353000	0.8544	413200
17	1.4120	0.9217	0.9708	340000	0.8618	394500
17.5	1.4360	0.9180	0.9680	325500	0.8673	375300
18	1.4540	0.9152	0.9658	311500	0.8712	357600
18.5	1.4720	0.9124	0.9635	296159	0.8748	338600
19	1.4850	0.9104	0.9619	282000	0.8773	321400
19.5	1.4960	0.9087	0.9605	269000	0.8793	305900
20	1.5050	0.9074	0.9594	256354	0.8810	291000
21	1.5170	0.9056	0.9578	234000	0.8831	265000
22	1.5250	0.9044	0.9568	217500	0.8844	245900
23	1.5320	0.9033	0.9559	203000	0.8856	229200
24	1.5370	0.9026	0.9552	191000	0.8864	215500
25	1.5410	0.9020	0.9547	180956	0.8871	204000
26	1.5435	0.9016	0.9543	171000	0.8875	192700
27	1.5405	0.9020	0.9547	164000	0.8870	184900
28	1.5475	0.9010	0.9538	158000	0.8881	177900
29	1.5495	0.9007	0.9535	152000	0.8885	171100
30	1.5500	0.9006	0.9535	148000	0.8885	166600
31	1.5500	0.9006	0.9535	145000	0.8885	163200
32	1.5465	0.9011	0.9539	140000	0.8880	157700
33	1.5400	0.9021	0.9548	136000	0.8869	153300
34	1.5360	0.9027	0.9553	132000	0.8863	148900
35	1.5315	0.9034	0.9559	128000	0.8855	144500
36	1.5260	0.9042	0.9566	125000	0.8846	141300
37	1.5200	0.9051	0.9574	122500	0.8836	138600
38	1.5140	0.9060	0.9582	121000	0.8825	137100
39	1.5100	0.9066	0.9587	121000	0.8818	137200
40	1.5060	0.9072	0.9592	122500	0.8811	139000
41	1.5030	0.9077	0.9596	124000	0.8806	140800
42	1.5020	0.9078	0.9597	124458	0.8804	141400
43	1.5020	0.9078	0.9597	123750	0.8804	140600
44	1.5030	0.9077	0.9596	122600	0.8806	139200
45	1.5060	0.9072	0.9592	121900	0.8811	138300
46	1.5100	0.9066	0.9587	122000	0.8818	138300
47	1.5120	0.9063	0.9585	122750	0.8822	139100
48	1.5150	0.9059	0.9581	123750	0.8827	140200
49	1.5225	0.9047	0.9571	124700	0.8840	141100

Table 1 (cont.)

λ [µm]	n	τ_{iso}	τ_o	a [m-1]	μ_d	K_d [m^{-1}]
50	1.5370	0.9026	0.9552	125161	0.8864	141200
51	1.5600	0.8991	0.9521	125100	0.8901	140500
52	1.5900	0.8947	0.9481	125050	0.8947	139800
53	1.6200	0.8904	0.9440	125025	0.8990	139100
54	1.6500	0.8861	0.9398	125000	0.9031	138400
55	1.6730	0.8828	0.9366	124900	0.9061	137800
56	1.6900	0.8804	0.9342	124000	0.9083	136500
57	1.7030	0.8786	0.9324	122500	0.9100	134600
58	1.7110	0.8775	0.9312	120700	0.9110	132500
59	1.7180	0.8765	0.9302	118700	0.9118	130200
60	1.7225	0.8759	0.9296	116600	0.9124	127800
61	1.7300	0.8748	0.9285	114500	0.9133	125400
62	1.7375	0.8738	0.9274	112500	0.9142	123100
63	1.7460	0.8727	0.9262	110700	0.9152	121000
64	1.7560	0.8713	0.9248	108800	0.9164	118700
65	1.7660	0.8699	0.9233	106900	0.9176	116500
66	1.7770	0.8684	0.9217	105000	0.9189	114300
67	1.7880	0.8670	0.9201	103100	0.9201	112000
68	1.7980	0.8656	0.9187	101200	0.9213	109800
69	1.8080	0.8643	0.9172	99500	0.9224	107900
70	1.8180	0.8630	0.9157	97800	0.9235	105900
71	1.8275	0.8617	0.9143	96100	0.9245	104000
72	1.8360	0.8606	0.9131	94600	0.9254	102200
73	1.8450	0.8594	0.9118	93100	0.9263	100500
74	1.8540	0.8582	0.9105	91600	0.9272	98790
75	1.8630	0.8571	0.9091	90000	0.9281	96970
76	1.8720	0.8559	0.9078	88600	0.9289	95380
77	1.8800	0.8549	0.9066	87200	0.9297	93790
78	1.8890	0.8537	0.9053	86000	0.9305	92420
79	1.8970	0.8527	0.9041	84600	0.9312	90850
80	1.9040	0.8518	0.9031	83400	0.9318	89500
81	1.9100	0.8511	0.9022	82100	0.9323	88060
82	1.9175	0.8501	0.9011	81000	0.9329	86830
83	1.9230	0.8494	0.9003	79800	0.9333	85500
84	1.9280	0.8488	0.8995	78750	0.9337	84340
85	1.9330	0.8482	0.8988	77750	0.9341	83240
86	1.9375	0.8476	0.8981	76750	0.9344	82140
87	1.9420	0.8470	0.8975	75800	0.9347	81100
88	1.9455	0.8466	0.8970	75000	0.9349	80220
89	1.9490	0.8462	0.8964	74000	0.9352	79130
90	1.9530	0.8457	0.8959	73200	0.9354	78250
91	1.9565	0.8452	0.8953	72300	0.9356	77270
92	1.9590	0.8449	0.8950	71450	0.9358	76350
93	1.9625	0.8445	0.8944	70600	0.9360	75430
94	1.9660	0.8441	0.8939	69800	0.9362	74560
95	1.9680	0.8438	0.8936	69000	0.9363	73700
96	1.9720	0.8433	0.8930	68100	0.9365	72720
97	1.9750	0.8429	0.8926	67200	0.9366	71750
98	1.9775	0.8426	0.8922	66450	0.9368	70940
99	1.9820	0.8421	0.8916	65600	0.9370	70010
100	1.9850	0.8417	0.8911	64717	0.9371	69060

Table 2. Integrated irradiance at different depths

	100 W		200 W		300 W	
Depth mm	E_d W m^{-2}	E_d %	E_d W m^{-2}	E_d %	E_d W m^{-2}	E_d %
0	1652	100.0 %	3715.6027	100.0 %	5774	100.0 %
0.01	692.7	41.92 %	1711.6578	46.07 %	2789	48.31 %
0.02	417.9	25.29 %	1108.9095	29.84 %	1884	32.63 %
0.03	278.1	16.83 %	785.70874	21.15 %	1385	23.99 %
0.04	196.6	11.90 %	588.43607	15.84 %	1074	18.60 %
0.05	145.4	8.800 %	459.24139	12.36 %	865	14.98 %
0.06	111.5	6.748 %	370.13774	9.962 %	717.8	12.43 %
0.07	88.02	5.326 %	306.08114	8.238 %	609.9	10.56 %
0.08	71.12	4.304 %	258.4404	6.956 %	528.1	9.146 %
0.09	58.58	3.545 %	222.00597	5.975 %	464.5	8.044 %
0.1	49.04	2.968 %	193.49251	5.208 %	413.9	7.168 %
0.2	14.58	0.8822 %	79.53972	2.141 %	198.5	3.438 %
0.3	7.669	0.4641 %	50.201313	1.351 %	134.6	2.332 %
0.4	5.174	0.3131 %	37.045133	0.9970 %	103.0	1.784 %
0.5	3.879	0.2347 %	29.180018	0.7853 %	83.01	1.438 %
0.6	3.052	0.1847 %	23.755926	0.6394 %	68.80	1.191 %
0.7	2.464	0.1491 %	19.741152	0.5313 %	58.09	1.006 %
0.8	2.024	0.1225 %	16.65242	0.4482 %	49.73	0.8613 %
0.9	1.685	0.1019 %	14.217202	0.3826 %	43.07	0.7459 %
1	1.418	0.08579 %	12.262824	0.3300 %	37.66	0.6522 %
2	0.3799	0.02299 %	4.0346428	0.1086 %	13.82	0.2394 %
3	0.1559	0.009433 %	1.903561	0.05123 %	7.068	0.1224 %
4	0.07755	0.004693 %	1.0695313	0.02878 %	4.278	0.07408 %
5	0.04338	0.002625 %	0.6788786	0.01827 %	2.916	0.05050 %
6	0.02682	0.001623 %	0.4762344	0.01282 %	2.177	0.03771 %
7	0.01818	0.001100 %	0.3617785	0.009737 %	1.738	0.03011 %
8	0.01335	0.000808 %	0.2914802	0.007845 %	1.453	0.02517 %
9	0.01045	0.000632 %	0.2446254	0.006584 %	1.253	0.02169 %
10	0.008553	0.000518 %	0.2110011	0.005679 %	1.102	0.01908 %
20	0.002641	0.000160 %	0.0786672	0.002117 %	0.4498	0.007790 %
30	0.001191	0.000072 %	0.0403662	0.001086 %	0.2468	0.004274 %
40	0.0006746	0.000041 %	0.0254481	0.000685 %	0.1634	0.002830 %
50	0.0004547	0.000028 %	0.0183526	0.000494 %	0.1213	0.002101 %

Table 3. Temperature increase in different layers

Depth interval	100 W	200 W	300 W
	dT/dt	dT/dt	dT/dt
mm	deg s^{-1}	deg s^{-1}	deg s^{-1}
0-0.01	22.94	47.90	71.34
0.01-0.02	6.569	14.41	21.64
0.02-0.03	3.34	7.725	11.92
0.03-0.04	1.949	4.715	7.45
0.04-0.05	1.223	3.088	4.991
0.05-0.06	0.8105	2.130	3.517
0.06-0.07	0.5617	1.531	2.579
0.07-0.08	0.4039	1.139	1.954
0.08-0.09	0.2996	0.8708	1.521
0-0.01	3.832	8.418	12.81
0.1-0.2	0.0824	0.2724	0.5147
0.2-0.3	0.0165	0.0701	0.1526
0.3-0.4	0.0060	0.0314	0.0756
0.4-0.5	0.0031	0.0188	0.0478
0.5-0.6	0.0020	0.0130	0.0340
0.6-0.7	0.0014	0.0096	0.0256
0.7-0.8	0.0011	0.0074	0.0200
0.8-0.9	0.0008	0.0058	0.0159
0-1	0.3946	0.8851	1.3710
1-2	0.0002	0.0020	0.0057
2-3	0.0001	0.0005	0.0016
3-4	$<10^{-4}$	0.0002	0.0007
4-5	$<10^{-4}$	0.0001	0.0003
5-6	$<10^{-4}$	$<10^{-4}$	0.0002
6-7	$<10^{-4}$	$<10^{-4}$	0.0001
7-8	$<10^{-4}$	$<10^{-4}$	0.0001
8-9	$<10^{-4}$	$<10^{-4}$	$<10^{-4}$
0-10	0.0561	0.0888	0.1380
10-20	$<10^{-4}$	$<10^{-4}$	$<10^{-4}$
20-30	$<10^{-4}$	$<10^{-4}$	$<10^{-4}$
30-40	$<10^{-4}$	$<10^{-4}$	$<10^{-4}$
40-50	$<10^{-4}$	$<10^{-4}$	$<10^{-4}$

Table 4. Ratio between ocean and tank scales

	Solar radiation in ocean	Infrared radiation in tank	Scaling ratio ocean / tank
	Depth	Depth	
50 % absorbed	1 m	0.01 mm	$1.0 \cdot 10^5$
99 % absorbed	25-90 m	0.2-0.7 mm	$1.2 \cdot 10^5$ - $1.3 \cdot 10^5$
Current towards Pole	200-500 m	2 cm	$1.0 \cdot 10^4$ - $2.5 \cdot 10^4$
Current towards Equator	1000-5000 m	2-8 cm	$5 \cdot 10^4$ - $6 \cdot 10^4$
Total depth to bottom	4000-5000 m	40 cm	$1.0 \cdot 10^4$ - $1.25 \cdot 10^4$

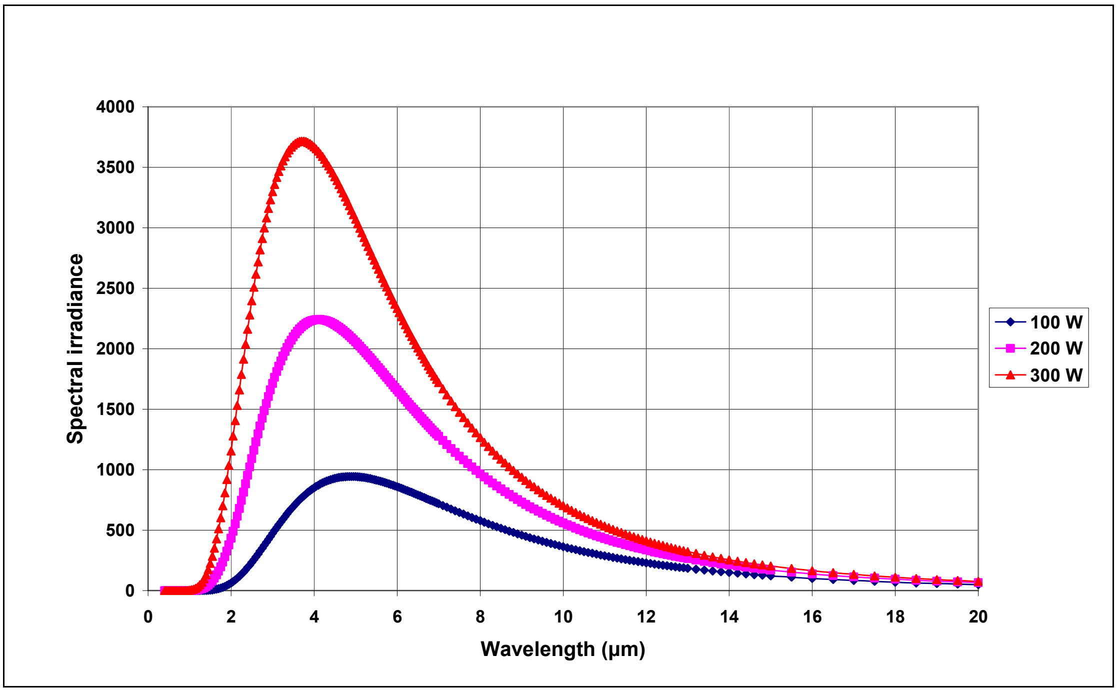

Fig. 1. The blackbody radiation of the lamp, shown as the spectral irradiance emitted by the heating element, in units of W m^{-2} μm^{-1}.

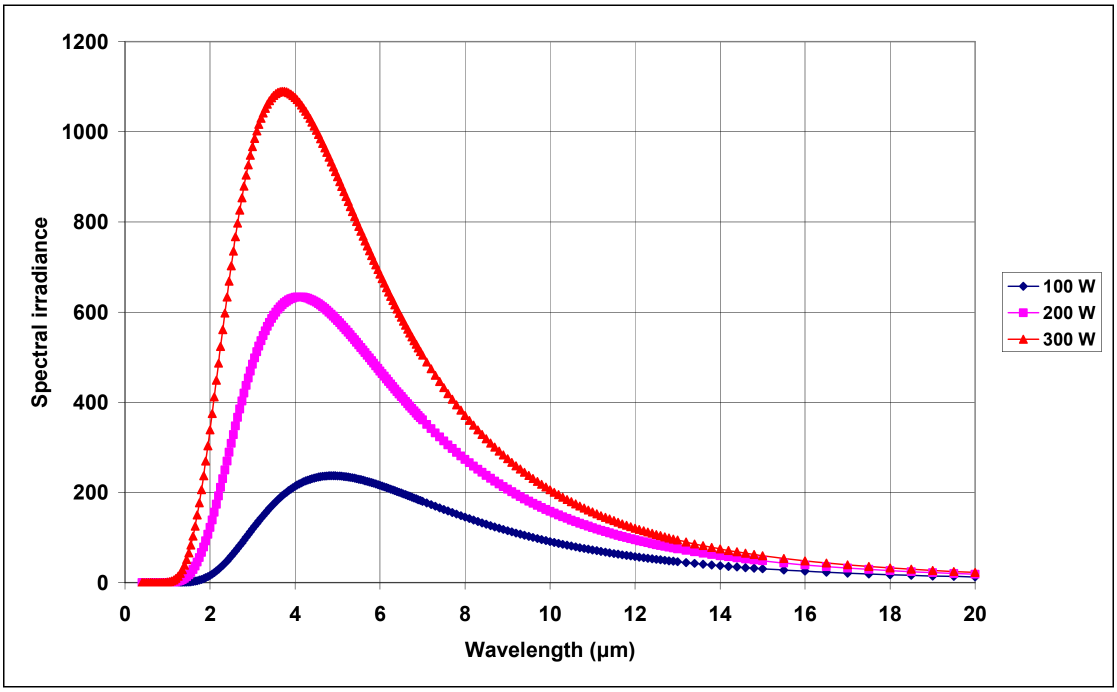

Fig. 2. Spectral downward irradiance from the lamp in units of W m^{-2} µm^{-1}, incident at the surface of the water.

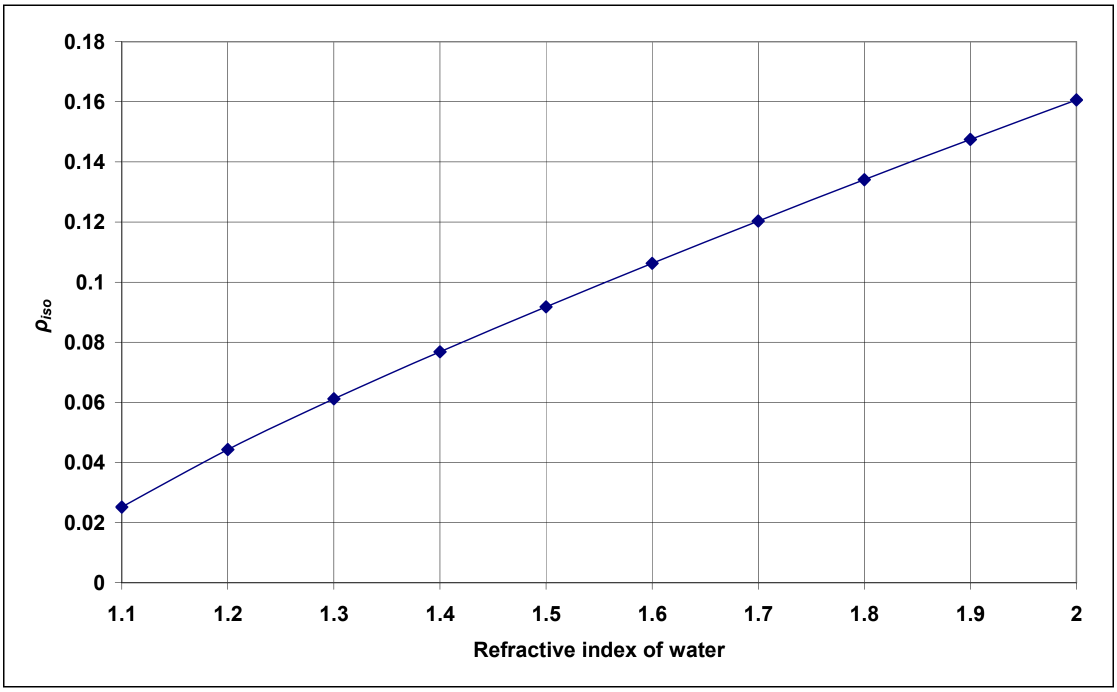

Fig. 3. Reflectance of irradiance at the surface of the water, as a function of the refractive index of water. The irradiance is assumed to consist of isotropic downward radiance.

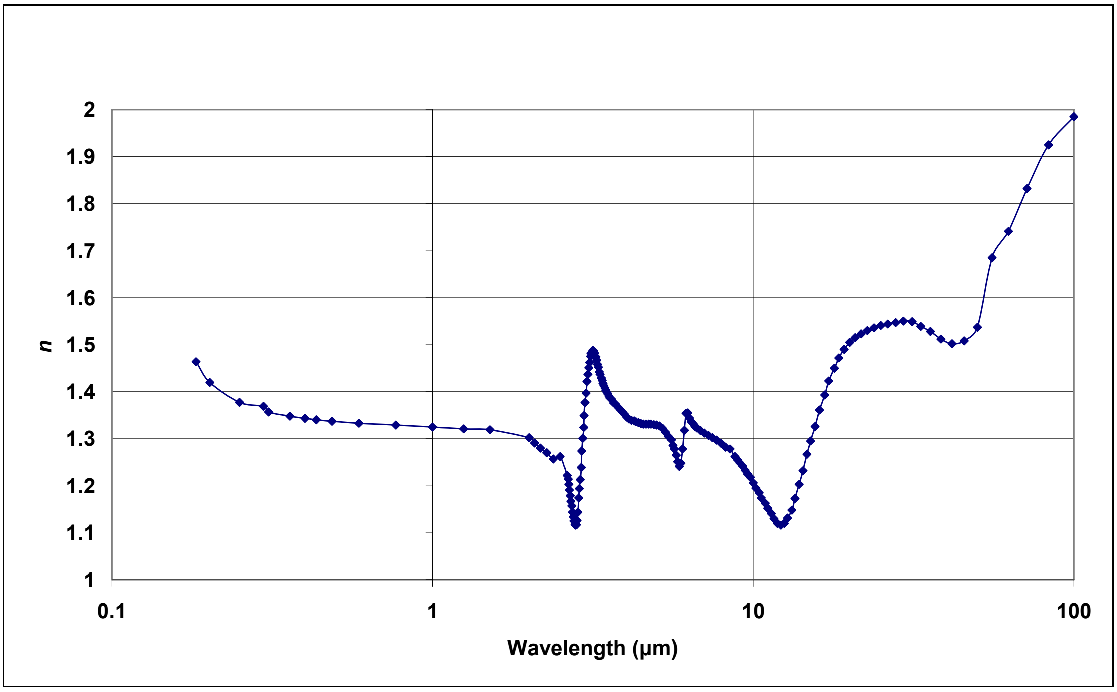

Fig. 4. Spectral variation of the refractive index of water.

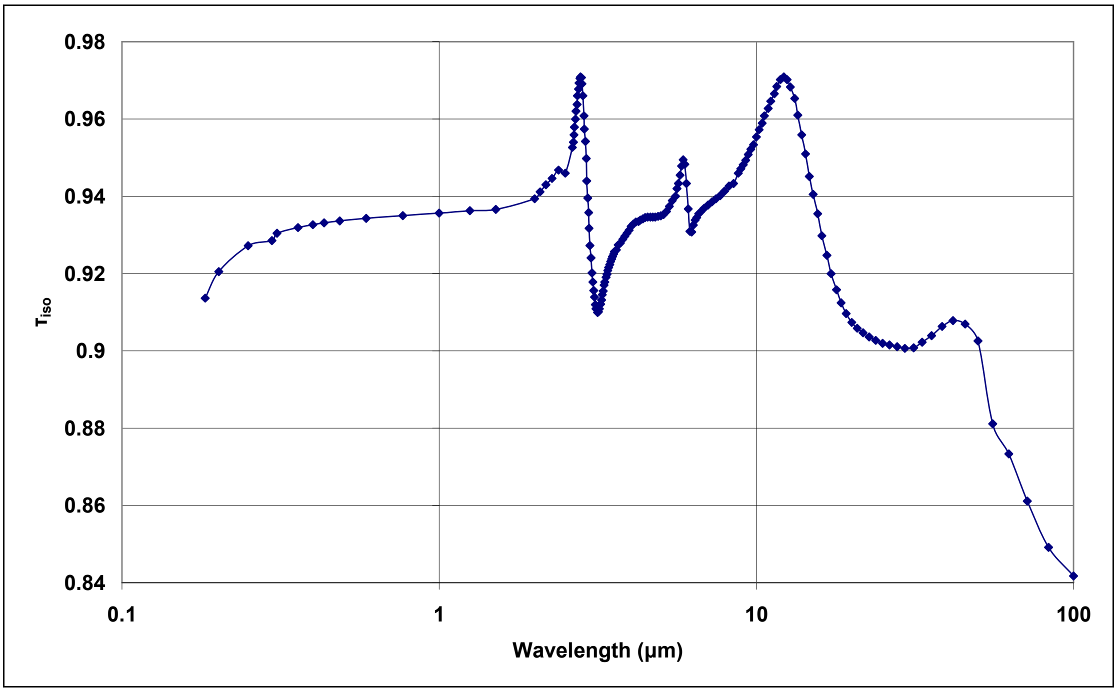

Fig. 5. Spectral variation of the transmittance of downward irradiance at the air-water interface. The irradiance is assumed to consist of isotropic downward radiance.

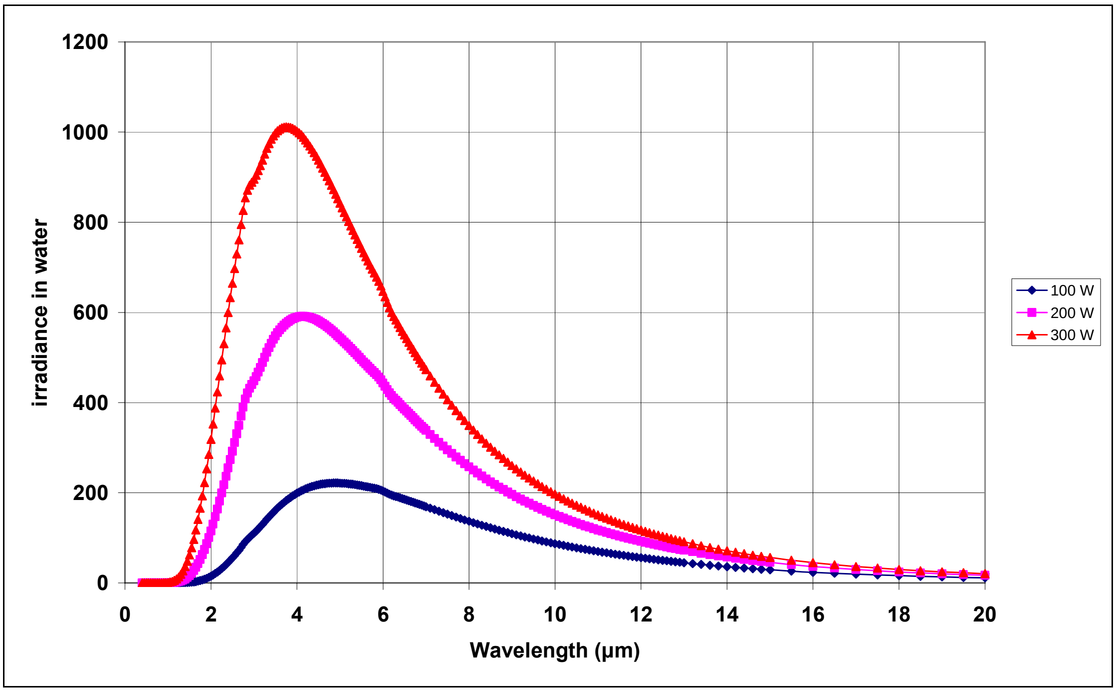

Fig. 6. Spectral downward irradiance just beneath the surface, in units of W m^{-2} μm^{-1}.

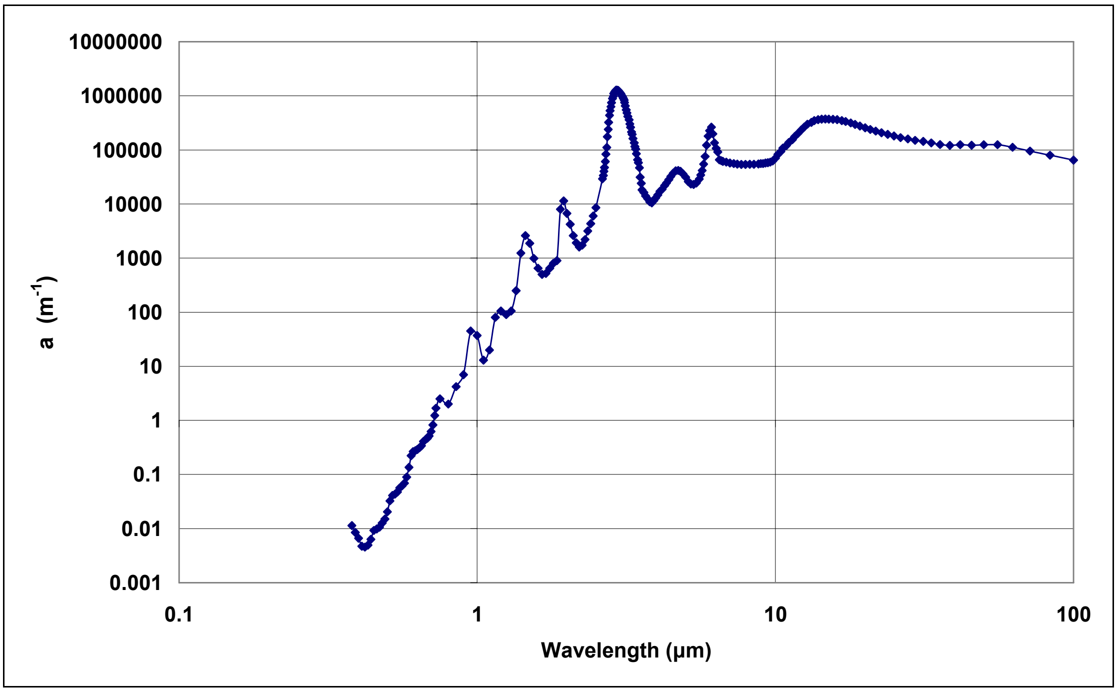

Fig. 7. Spectral variation of the absorption coefficient of pure water.

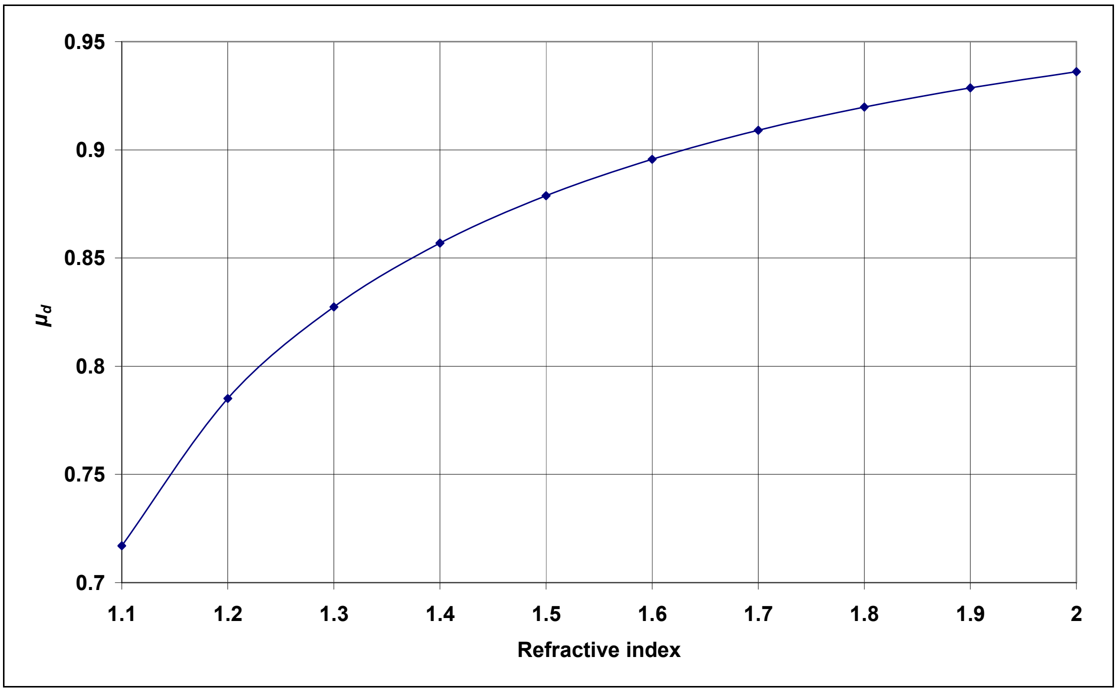

Fig. 8. The average cosine of downward radiance just beneath the surface, as a function of the refractive index of water.

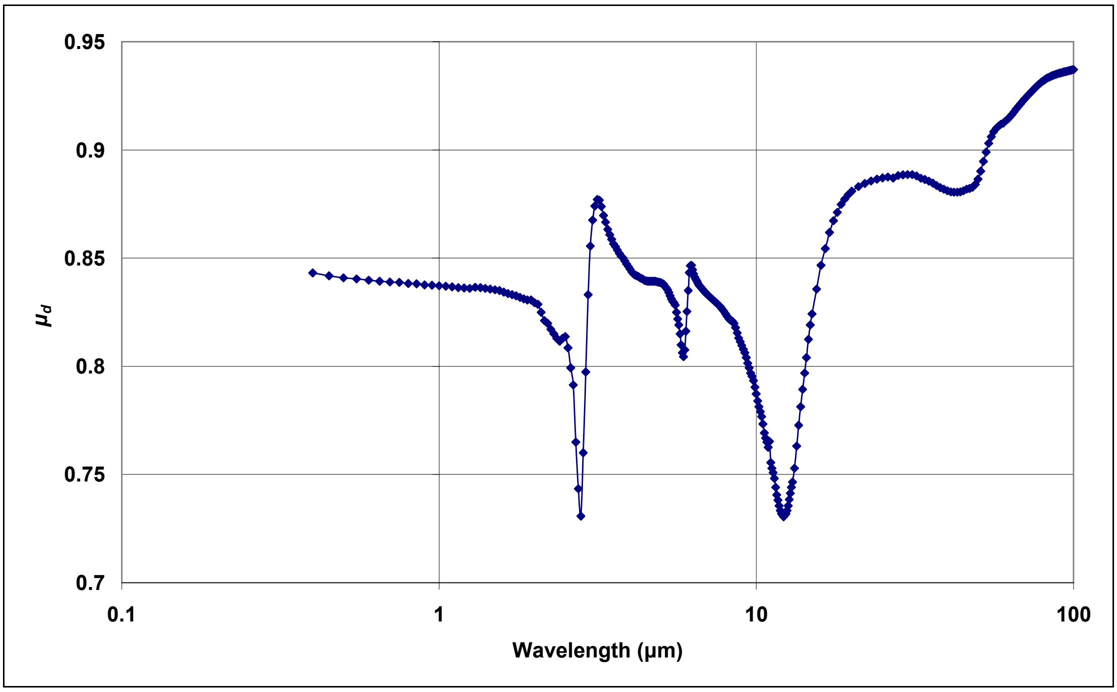

Fig. 9. Spectral variation of the average cosine of downward radiance just beneath the surface.

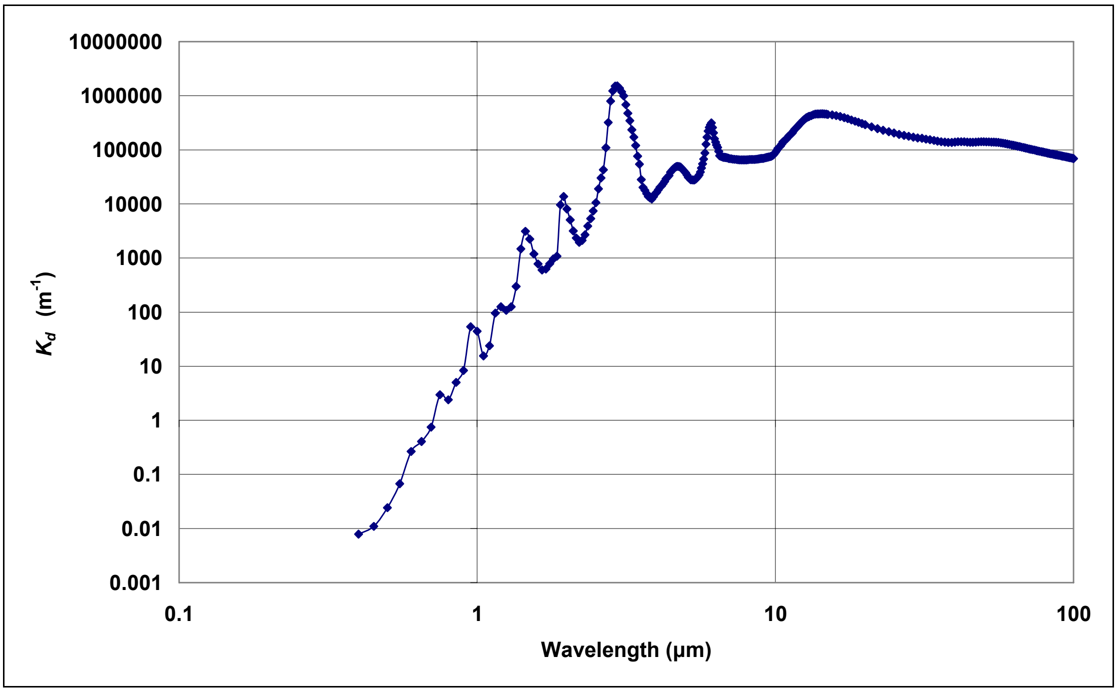

Fig. 10. Spectral variation of the vertical attenuation coefficient of downward irradiance.

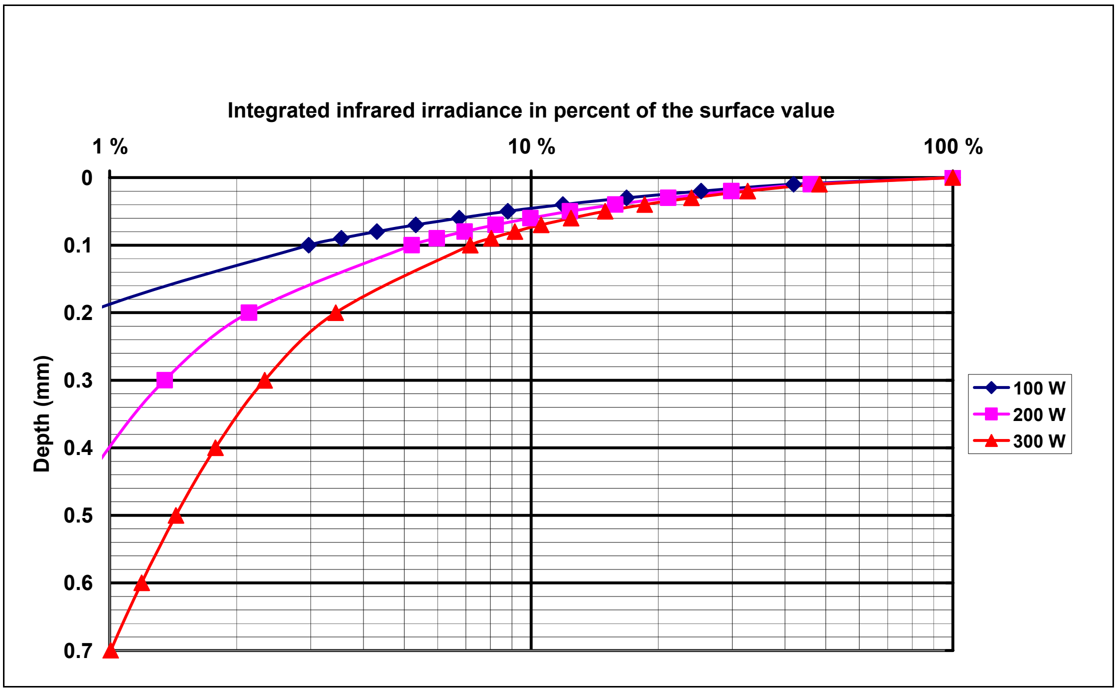

Fig. 11. Integrated downward irradiance as a function of depth.